THE RESPONSE OF A FABRY-PEROT OPTICAL CAVITY TO PHASE MODULATION SIDEBANDS FOR USE IN ELECTRO-OPTIC CONTROL SYSTEMS

Kenneth D. Skeldon and Kenneth A. Strain

Department of Physics and Astronomy, University of Glasgow, G12 8QQ, Scotland.

Abstract

The worldwide endeavour to build long baseline laser interferometers to detect and study gravitational radiation is well underway. In the German-British GEO 600 project, it is proposed to pass the sidebands induced on the light by an electro-optic phase modulator through a Fabry-Perot optical cavity used in transmission, called a modecleaner. This can be achieved by arranging for the phase modulation frequency to match the first longitudinal mode frequency of the modecleaner cavity, so that both carrier and sidebands are transmitted. The primary function of the modecleaner is to reduce the geometry fluctuations associated with the light, and thus any such noise induced by the modulation process is also suppressed. We present the results of an experiment that investigates the feasibility of passing modulation sidebands through an optical cavity, and the factors limiting its success. In particular, we show that it is possible to avoid introducing excess noise associated with the transmitted sidebands, provided that certain experimental criteria are satisfied. The work was carried out on a prototype modecleaner cavity built and tested at Glasgow University, but similar to the equivalent apparatus planned for GEO 600.

keywords: gravitational waves, modulation, modecleaner.

1 Introduction

The German-British 600 m arm length laser interferometer GEO 600, is currently being built near Hannover. When completed early next century, it is

anticipated that GEO 600 should be able to detect gravitational radiation from violent events happening in the universe, by measuring tiny differential optical path length changes induced by the passing waves. In a system like GEO 600, there are several noise sources that have to be reduced before the interferometer can reach an astronomically useful sensitivity. One of these sources of noise is geometry fluctuations associated with the laser light.[1] These fluctuations can be modelled as small contributions of high order transverse laser modes being added to the fundamental mode.[2,3] A convenient way of reducing beam geometry noise is to use a non-confocal Fabry-Perot optical cavity in transmission, locked to the fundamental mode of the laser, so that the higher order modes are off-resonant and are suppressed. Such a Fabry-Perot system is known as a modecleaner. In order to achieve the required level of beam geometry noise suppression in GEO 600, the modecleaner scheme will consist of two optical ring cavities arranged one after the other in in the beam path from the laser to the interferometer.

Normally, the beam geometry fluctuations that must be suppressed are those in the detection bandwidth, say around 10 Hz to 1 kHz. However another important function provided by the modecleaners is to suppress beam position fluctuations induced by the electro-optic phase modulators used in GEO 600. However, the number of modulators that can be placed before the modecleaners is restricted to one for the following reason: by choosing to place a given modulator before the modecleaners, we immediately define the frequency of that modulator to be an integral number of the frequency spacing between longitudinal resonances, or free spectral range (FSR), associated with the modecleaner cavities. Since all modulation frequencies are necessarily distinct, and should not be harmonics of one another, this limits the number of pre-modecleaner modulators to one. Furthermore, since it is unwise to have the FSRs of each modecleaner identical, the modulator must be placed between the modecleaner cavities so that the frequency of the induced sidebands is matched to the FSR

of the second modecleaner only. In GEO 600 it is intended to pass one of the most important modulation frequencies, that used to control the power recycling cavity, through the second modecleaner.

2 Modecleaners and modulation frequencies

The properties of optical modecleaners have been well documented in various publications.[3,4] The advantages of using them over other methods of beam geometry noise reduction stems primarily from the availability of very low loss mirrors. These optics can be used to construct a high finesse optical cavity with very good power handling capability, and efficient light power throughput, while the small linewidth makes for a useful low-pass filtering action that will passively suppress other types of laser noise including power and frequency noise.

Each modecleaner cavity in GEO 600 will support various longitudinal and transverse laser modes (TEM modes), each having a different frequency of resonance within the cavity. For a cavity having two mirrors, with radius of curvatures R_1, R_2 separated by a distance L, the frequency f_{nmq} for the mode TEM_{nmq} is given by[5]

$$f_{nmq} = \left[(q+1) + \frac{1}{\pi}(n+m+1)\cos^{-1}\left(\sqrt{1-\frac{L}{R_1}}\sqrt{1-\frac{L}{R_2}}\right)\right] FSR \qquad (1)$$

where n, m are the transverse mode numbers, q is the longitudinal mode number and FSR is the free spectral range of the cavity given by $FSR = c/(2L)$. For a given pair of transverse mode numbers, there are multiple longitudinal resonances offered by each value of q, available in practice by altering the cavity round-trip length by one wavelength of the light at a time. In normal operation each modecleaner would be locked to the fundamental mode of the light, TEM_{00}, effectively fixing a value for q, whereupon the modes with higher values of $(n+m)$, and indeed different values of q, would be offset from resonance by

an amount Δf_{nmq} given by

$$\Delta f_{nmq} = \Delta q \frac{c}{2L_j} + (n+m)\frac{c}{2\pi L_j}\cos^{-1}\left(\sqrt{1-\frac{L_j}{R_1}}\sqrt{1-\frac{L_j}{R_2}}\right) \qquad (2)$$

where L_j is appropriate to the j^{th} modecleaner ($j = 1, 2$). In GEO 600 we have decided it advisable that all the modulation frequencies, except the one chosen for passage through the second modecleaner, should differ in value from those that could give rise to coupling between a modulation sideband and a cavity mode. In other words we should strive for

$$M_i \neq \left[\Delta q + \frac{1}{\pi}(n+m)\cos^{-1}\left(\sqrt{1-\frac{L_j}{R_1}}\sqrt{1-\frac{L_j}{R_2}}\right)\right] FSR_j \qquad (3)$$

where $M_i = \{M_1, M_2, ..., M_r\}$ represents the set of modulation frequencies chosen for the various control systems employed up to and including the second modecleaner in the GEO 600 system. One member of this set, say M_r, will not obey this inequality and will have its value defined as FSR_2. Further to the above constraint on M_i, we have also insisted that the first few harmonics of M_i satisfy the inequality also. The safety margin between M_i or harmonics of M_i, and the various cavity mode frequencies has been taken to be ten linewidths of each modecleaner cavity, by which stage any signal coupling into the cavities would be reduced by 120 dB through passive filtering alone. As indicated above, low loss mirrors permit high values of light power throughput to be achieved while also allowing narrow linewidths for the modecleaners, making it easier to satisfy Eqn.(3) for all M_i and first few harmonics, say up to $7M_i$. The mirror properties of each modecleaner are identical, and they differ only in their lengths, and hence their FSRs and mode spacings. The important parameters are given in Table 1. We should point out that both GEO 600 modecleaners are triangular ring cavities having two closely spaced flat mirrors and a distant 6 m curved mirror. The equivalent two mirror cavity configuration is then $R_1 = 6$ m, $R_2 = \infty$ and $L_j = d_j/2$ where d_j is the round trip optical path length within the j^{th} modecleaner, listed in Table 1.

In addition to the cavity mode considerations, we also impose the condition that potential beating between modulation frequencies should not lie within the bandwidth of any of the GEO 600 control systems. Given that the maximum bandwidth of any of the GEO 600 control systems is likely to be of order 1 MHz, we have the additional criterion $|M_a - M_b| > 10^6$ that must be satisfied for all $1 < a, b < r$ $(a \neq b)$. It is proposed that the source producing M_r be regarded as a master oscillator in GEO 600 with all other modulation frequencies $M_1, ..., M_{r-1}$ phase locked to M_r.

3 Description of an experimental test of modecleaner response to modulation sidebands

Although in theory it should be possible to transmit modulation sidebands through a modecleaner, it is instructive to consider the practical factors that may exist to limit the success of such a proceedure. The modulation sidebands that are to be transmitted through MC2 can be regarded as independently applied to the light, and thus will not follow changes or drifts in operating conditions associated with the main control systems that keep the cavity on resonance with the light. It is possible that changes in cavity alignment or loop gain variations may affect the transmitted sidebands. Such concerns are relevant not only in GEO 600 but in all the long-baseline interferometers around the world, currently encompassing the American LIGO, French-Italian VIRGO and Japanese TAMA projects. Experiments designed to address the issues have been performed by these groups and some have been summarised in internal project papers. Here we describe and report the results of a series of experiments on the Glasgow modecleaner which was developed primarily as a prototype cavity for the modecleaner system planned for GEO 600.[6]

The experimental arrangement in shown in Fig 1. The modecleaner cavity contains four suspended fused-silica masses with attached mirrors. The masses are damped using a local control system for each. The local controls also allow

the masses to be rotated and tilted to permit manual alignment of the cavity with respect to the ingoing light. The modecleaner round-trip distance was measured to be about 16.8 m implying a longitudinal mode spacing of around 17.85 MHz. The laser used is an argon ion laser operated at 514.5 nm and a power specification of around 1 W single mode. The laser light passes through two EOM units on its way to the modecleaner. The first EOM is fed from a variable frequency oscillator to allow the modulation frequency to be varied through the FSR of the modecleaner. The modulator used was an Electro-Optic Developments model PC 14 which has an active length of 6.5 cm giving it a relatively low half-wave voltage of 85 V. We shall refer to the modulation frequency associated with this modulator as f_1. The second EOM, a Gsänger PM 25, applies modulation sidebands at 10 MHz which, in conjunction with the reflected cavity signal at PD2, allows the locking of the laser to the modecleaner using the rf-reflection technique.[7,8] This modulation is also used in an automatic alignment system that keeps the modecleaner optimally aligned to the ingoing light. This is achieved by sensing the lateral and angular drift in the reflected light using the photodiode array containing PD3 and PD4, and then deriving suitable control signals which are used to rotate and tilt the input and output mirrors to correct for these drifts.[9,10] During the experiment, the best visibility obtainable manually was around 75 %, and the auto-alignment system held this value when switched on.

The variable modulation was applied using a Marconi digital rf generator matched into a 1 W amplifier and this in turn feeding a resonant LC voltage multiplier circuit with the EOM providing the C. The arrangement is shown in Fig 2 along with the tuning curve of the circuit based on a set of experimental measurements taken using a Tropel scanning cavity to investigate the sideband height relative to the carrier. For the purposes of our experiment it is important that the linewidth of the resonant circuit powering the EOM is far greater than the linewidth of the modecleaner so that the amplitude of the applied sidebands

remains constant during a frequency sweep through the modecleaner resonance. This simplifies diagnostics regarding the effect of the cavity response on the sideband amplitudes.

In general, a light field that has modulation sidebands applied can be described by

$$E = [J_0(\beta) + J_1(\beta)\exp(i\omega_m t) - J_1(\beta)\exp(-i\omega_m t)]\, E_0 \exp(i\omega t) \qquad (4)$$

where ω is the carrier frequency of the light, ω_m is the modulation frequency, β is the modulation index, E_0 is the amplitude of the light field before modulation and J_0, J_1 are the Bessel functions of 0^{th} and 1^{st} order. The light field at PD1 in Fig 1 depends on the back-reflected light from the cavity which will consist of two contributions; the first is a directly reflected beam from the back surface of the input mirror which we will denote E_r, and the second is the light that leaks back out of the cavity after undergoing several round-trips inside the cavity, which we will call E_l. If we neglect the reduction in carrier power due to the 10 MHz modulation and consider only the effect of the modulation applied at f_1, then these reflected fields can be described by

$$E_r = [J_0(\beta_1) - J_1(\beta_1)\exp(i\omega_1 t) + J_1(\beta_1)\exp(-i\omega_1 t)]\, E_0 \qquad (5)$$

$$\begin{aligned} E_l \;=\; & [\, J_0(\beta_1)\frac{T\rho\exp(i\phi_1)}{1-\rho\exp(i\phi_1)} + J_1(\beta_1)\frac{T\rho\exp(i[\phi_1+\phi_2])}{1-\rho\exp(i[\phi_1+\phi_2])} \\ & -J_1(\beta_1)\frac{T\rho\exp(i[\phi_1-\phi_2])}{1-\rho\exp(i[\phi_1-\phi_2])}\,]\, E_0 \end{aligned} \qquad (6)$$

where $\omega_1 = 2\pi f_1$, β_1 is the modulation index for the applied modulation at f_1, T is the power transmittance of the input mirror, $\rho = (R_1, \ldots R_n)^{\frac{1}{2}}$ where $R_1, \ldots R_n$ are the power reflectances for each mirror in the modecleaner. ϕ_1 is the phase offset acquired in a round trip of the cavity due to f_1 not exactly matching FSR, and ϕ_2 has the same interpretation for the carrier itself, due to offsets, or lack of gain in the laser frequency stabilisation scheme. There should be an input mirror reflectance coefficient in Eqn.(5), however for high reflectance

mirrors we can approximate this to unity. In terms of the frequencies ω_1 and ω_2, where ω_2 is the frequency offset from resonance due to imperfections in the stabilisation loop, we can write $\phi_1 = \omega_1/FSR$ and $\phi_2 = \omega_2/FSR$. The signal V_Q observed at point Q in Fig 1 is that measured by PD1 and then demodulated at f_1. This can be calculated by extracting the terms with coefficient $e^{i\omega_1 t}$ in

$$I_1 = (E_r + E_l)(E_r + E_l)^* \tag{7}$$

which, after some considerable expansion and simplification, can be written as

$$\begin{aligned} V_Q &= 2ATJ_1(\beta_1)\left(\frac{2F}{\pi}\right)^2 \\ &\times \left[\frac{J_0(\beta_1)\sin\phi_1}{1+\left(\frac{2F}{\pi}\right)^2\sin^2\frac{\phi_1}{2}} + \frac{J_1(\beta_1)\sin(\phi_2+\phi_1)}{1+\left(\frac{2F}{\pi}\right)^2\sin^2\left(\frac{\phi_2+\phi_1}{2}\right)} + \frac{J_1(\beta_1)\sin(\phi_2-\phi_1)}{1+\left(\frac{2F}{\pi}\right)^2\sin^2\left(\frac{\phi_2-\phi_1}{2}\right)}\right] \end{aligned} \tag{8}$$

where F is the finesse of the cavity, given approximately by $F \approx \frac{1}{1-\rho}$, and A is a constant depending on the signal strengths. This expression is the mathematical description of the error signal that is obtained from an rf reflection locking scheme with demodulation frequency f_1, however with the added effect of an additional phase offset from resonance for the carrier resonance given by ϕ_2.

4 Experimental aspects of the modecleaner response to modulation sidebands

The signals of primary interest in the experiment are those measured at P and Q, denoted by V_P and V_Q respectively. The signal V_P is the laser power transmitted through the cavity, measured with a broadband photodiode. To begin with this signal will be investigated at the modulation frequency f_1. Following this, it will be demodulated with a local oscillator derived from f_1 and the spectrum of the result will be analysed from DC up to a few hundred Hz.

As discussed above, V_Q is the light reflected from the cavity measured by PD1 and demodulated at f_1 and will show a dependency on both the carrier

offset from resonance and the modulation frequency offset from the modecleaner FSR. Both these effects are described by Eqn.(8).

4.1. Investigation of the transmitted light at the modulation frequency f_1

It is possible to use V_P to provide information about when f_1 matches the cavity FSR. In the first instance, V_P was measured with a high-frequency spectrum analyser while f_1 was varied over a range of several hundred Hz on either side of the cavity FSR. The component of V_P at f_1, which can be regarded as the amplitude modulation imposed at f_1 on the throughput light, was plotted as a function of f_1 and is shown in Fig 3. The minimum value occurs when $f_1 = FSR$, and provides a direct measurement of the FSR. At frequencies on either side of this minimum the modecleaner converts the frequency sideband Fourier components into even greater amplitude modulation on the transmitted light, since the sidebands get reflected from the cavity in accordance with the modecleaner resonance curve; this curve provides the characteristic shape of the central dip in Fig 3. The finesse of the modecleaner was measured to be around 600 corresponding to a linewidth of around 30 kHz, which is in good agreement with the value suggested by Fig 3. The shape of the plot in Fig 3 at frequencies further away from the central dip is determined by the tail of the cavity response combined with the tuning curve of the modulator circuit shown in Fig 2.

It is promising that the character of the sidebands when $f_1 = FSR$ is identical before and after the modecleaner, as demonstrated by the scans shown in Fig 4. These were taken with a Tropel scanning Fabry-Perot frequency discriminator.

A fact of particular interest here is whether or not the minimum value of V_P in Fig 3 represents the same relative amplitude modulation on the throughput light as that measured on the ingoing light to the modecleaner. It would be desirable that the modecleaner should not impose any extra amplitude modulation on the light, provided that the condition $f_1 = FSR$ could be maintained.

The amplitude modulation at f_1 on the light power entering the modecleaner was typically 2×10^{-4}, being induced by polarisation noise at the EOM coupling to amplitude modulation through subsequent optical components having polarisation sensitivity. The polarisation noise associated with the EOM is highly temperature dependent and the level of amplitude modulation was sometimes seen to drift over timescales of minutes. For this reason, comparison measurements on the light entering and exiting the modecleaners were performed within a few seconds of each other.

Initially, the level of AM on the signal at P was seen to be a few times worse than the corresponding AM measured for the input light. However, an improvement in the frequency stabilisation circuitry, giving a few dB more gain up to several kHz, permitted the reduction of the AM at P to a level comparable with the AM on the incident light: around 2×10^{-4} at f_1 also. If the gain of the stabilisation control loop was reduced, then in general this level of AM could not be achieved. These measurements were performed with the auto-alignment control loop switched on. An interesting effect was noted if the alignment of the cavity was manually adjusted. By deliberating misaligning the cavity slightly, it was possible to actually reduce the level of AM measured at P to a value below that measured for the incident light: down to around 4×10^{-5} with care. This is most likely due to the misalignment generating a high order transverse mode which couples into AM within the cavity, and then this adds out of phase to the AM associated with the incident light.

42. Investigation of the transmitted light demodulated at the modulation frequency f_1

Having studied the level of AM associated with the signal at P at frequency f_1 we now investigate V_P demodulated with respect to f_1 and examined over a given frequency range. For gravitational wave interferometers, we are interested particularly in noise from a few tens of Hz to a few kHz. The demodulated spectrum is a particularly relevant measurement because it helps determine the suit-

ability of the modulation process at f_1 for an electro-optic control system where any excess noise introduced by the cavity would be undesirable. In GEO 600 it is anticipated that the locking of the power-recycling cavity will rely on the modulation applied at f_1. Fortunately however, the GEO 600 control topology is such that the feedback loop locking the power-recycling cavity to the light can tolerate a much greater level of noise around the modulation frequency f_1 than say, a loop which is related to the actual interferometer feedback signal, which would carry information about passing gravitational waves. Thus we make the measurement here, primarily to ensure that the level of noise associated with the demodulation of the light amplitude signal after the modecleaner is not considerably greater than that associated with the equivalent measurement made for the light entering the modecleaner cavity. The experimental proceedure is shown in Fig 5. The light before and after the modecleaner is examined using a revised photodiode circuit designed to be optimally sensitive to light noise at the modulation frequency with gain approaching zero towards DC. The DC light level could be conveniently monitored by measuring the voltage developed across the 1 mH inductor which has a resistance of around 0.7 Ω. The signal from the photodiode circuit is demodulated with a local oscillator derived from the signal generator used to drive the modulator circuit at frequency f_1. The demodulated signal is then investigated using a low-frequency spectrum analyser.

Initially, the background noise level associated with the signal after the modecleaner was found to be higher than the comparable measurement made for the light entering the modecleaner. In more detail, the noise level associated with the input light was consistent with the shot noise corresponding to the 25 mW of light falling on the photodiode. However the noise level of the light exiting the modecleaner was around 10 dB higher up to 100 Hz. thereafter falling to a level comparable with the input light noise.

The reason for the excess noise at low frequency was thought most likely to

be a combination of three principal factors. The first mechanism is modecleaner mirror motion in turn producing a fluctuating FSR, and hence providing direct coupling of the phase sidebands at f_1 to light power noise at f_1 associated with the throughput light. The second important factor is phase noise intrinsic to the rf generator used to apply the modulation sidebands. The modecleaner cavity will convert such phase noise into light power noise on the throughput light. The third consideration, which has an impact on the previous two factors, is concerned with the laser stabilisation scheme that keeps the laser locked to the modecleaner cavity; insufficient gain in this feedback system, especially in the frequency band of interest, would cause the sidebands at f_1 to fluctuate around the FSR of the cavity. The consequence of f_1 not being matched to the cavity FSR is that the power noise coupled in by the first two factors will then increase, according to the gradient of the cavity resonance curve shown in Fig 3. This effect could be produced experimentally by deliberately offsetting the value of f_1 from the cavity FSR by adjusting the frequency of the Marconi rf signal generator; for example an offset of just 100 Hz would produce an increase in the demodulated signal of just over 10 dB. We should also point out that the level of excess noise was also seen to be dependent on, although not very sensitive to, the alignment of the modecleaner. For example, the effects of drifts in visibility of around a few percent were just beginning to become noticeable on the throughput noise trace, however the problem was removed altogether in the presence of the auto-alignment scheme.

In order to address the excess noise problem two steps were taken. Firstly, the Marconi rf signal generator was replaced with a Hewlett Packard HP 8648A synthesizer having a very favorable documented specification regarding phase and amplitude noise. Secondly, the laser stabilisation scheme was improved further to increase the gain at low frequency, producing an open loop gain of $\sim 10^6$ at around 10 Hz. The change of rf generator had a noticeable effect on the level of noise associated with the demodulation of the light before the

modecleaner, the background being 10 dB lower up to several hundred Hz. This constitutes an experimental confirmation that the new HP synthesizer has lower noise specification than the Marconi unit, at least for amplitude noise.

With these measures we have been able to achieve a level of noise associated with the light exiting the modecleaner which is comparable with that measured for the input light at all but very low frequency. A comparison between two measured traces is shown in Fig 6. The excess noise below around 10 Hz is most probably due to seismic motion of the modecleaner mirrors. We have measured the ground motion around the modecleaner vacuum tanks using a seismometer, and also spectrum analysed the local control signals that damp the modecleaner masses. The spectra of each of these measurements have revealed structure characteristics that correlate with the low frequency part of the trace associated with the light after the modecleaner in Fig 6. In view of the results of Fig 6, it seems reasonable to suggest that the transmitted sidebands would be acceptable for use, even in a control system where there is a rather lower tolerance of noise around the modulation frequency than for the power-recycling control loop in GEO 600.

43. Investigation of the reflected light and its relevance to thermally induced offsets

We recorded an important feature during our experiments regarding temperature drifts in the operating environment each time the equipment was turned on for the first time each day. The modulation frequency f_1 had to be retuned typically by around 600 Hz in the morning, and then slowly decreased during the day as the apparatus, and the laboratory itself, became warmer. This retuning is necessary to correct for the drift in the round trip length of the cavity, caused by thermally induced stress associated with the vacuum chamber. An increase in the FSR of 600 Hz, which is around 2 % of the cavity linewidth, equates to a 0.56 mm decrease in round trip distance, or a 0.14 mm reduction in the nominal physical spacing between the mirrors. From Fig 3 it can be seen

that an offset of 600 Hz from the FSR of the cavity represents a rather large increase in the value of AM associated with the light at P. The exact increase is rather difficult to determine from the graph, but inspection of the experimental data points suggest that it is around a factor of 5. In addition, there is the issue of introducing excess noise associated with the demodulation of the throughput light with respect to f_1, described above. Therefore if such thermally induced effects are as evident in GEO 600 it may be necessary to correct for them either by tracking the cavity length to regulate the FSR, or else by feeding back to a VCO to alter the value of f_1.

In order to do this we must be able to generate an error signal and such a signal can be derived from V_Q in Fig 1. The plot shown in Fig 7(a) shows the form we would expect for V_Q as a function of the modulation frequency, based on Eqn.(8). The plot shown in Fig 7(b) is based on a set of experimental measurements of V_Q as f_1 is varied in steps of ± 100 Hz on either side of the cavity FSR. The position of the null of the AM measured at P, and hence the cavity FSR, corresponds to $f_1 = 17.8496$ MHz for this plot. The suitability of the signal V_Q as the source of a control signal, should it be required, is evident from these plots. The exact location of the null in the measured error signal at Q depends on ϕ_2, the carrier frequency offset from resonance. Thus in practice it is advisable to keep the offsets in this loop as low as possible.

5 Conclusion

We have investigated the practical considerations of passing phase modulation sidebands through a Fabry-Perot optical cavity. This process is important for the modecleaner scheme in the GEO 600 gravitational wave detector, where it is planned to pass modulation sidebands through such a cavity. Based on the experiments performed on the Glasgow prototype modecleaner, we have managed to reduce the level of AM on the throughput light to the equivalent level measured on the incident light. We have also investigated the demodulation

of the throughput light power noise over a bandwidth of a few hundred Hz, and found that we can eliminate excess noise introduced by the modecleaner at all frequencies above $\sim 10\,\mathrm{Hz}$ subject to there being sufficient gain at low frequency in the feedback system used to lock the laser to the modecleaner cavity. It has been pointed out that both these results are subject to various operating conditions. One of these conditions is that the modecleaner must be reasonably well aligned, at least to within the capabilities of auto-alignment control schemes such as the one implemented here. In addition, the FSR of the cavity must not drift with respect to the modulation frequency by more than a small fraction of the cavity linewidth. We found that thermal drifts in the cavity length amounting to a 600 Hz change in the FSR caused the level of AM on the output light to increase by almost a factor of 5 while an offset of 100 Hz caused the noise associated with the demodulated throughput light to increase by over 10 dB. The implication for GEO 600 is that control over such drifts may need to be employed, and we have shown that the necessary error signal for this can be obtained from the demodulated signal corresponding to the reflected light from the cavity.

Acknowledgements

We would like to thank the other members of the gravitational waves group at Glasgow for their general help and interest during this work. We must also thank the University of Glasgow and the UK Particle Physics and Astronomy Research Council (PPARC) for providing financial backing to allow these experiments to be performed. One of us, K.D. Skeldon, is funded from a PPARC Post Doctoral Research Fellowship award, while K.A. Strain is in receipt of a PPARC Advanced Research Fellowship award.

References

1. K. Skeldon and J. Hough, "Measurements of beam geometry fluctuations of

typical argon ion and Nd:YAG lasers with relevance to laser interferometer gravitational wave detectors," Rev. Sci. Instrum. **66**, 2760-2762 (1995).

2. D. Z. Anderson, "Alignment of resonant optical cavities," Appl. Opt. **23**. 2944-2949 (1984).
3. A. Rudiger, R. Schilling, L. Schnupp, W. Winkler, H. Billing and K. Maischberger, "A mode selector to suppress fluctuations in laser beam geometry," Opt. Acta. **28**, 641-658 (1981).
4. K. D. Skeldon, "Aspects of improvement in the sensitivity of long-baseline laser interferometric gravitational wave detectors," PhD thesis, Uni. Glasgow (1996).
5. H. Kogelnik and T. Li, "Laser beams and resonators," Proc. IEEE. **54**, 172-189 (1966).
6. K. D. Skeldon, K. A. Strain, A. I. Grant and J. Hough, "Test of an 18 m long suspended modecleaner cavity," Rev. Sci. Instrum. **67**, 2443-2448 (1996).
7. R. W. P. Drever, J. L. Hall, F. V. Kowalski, J. Hough, G. M. Ford, A. J. Munley and H. Ward, "Laser phase and frequency stabilisation using an optical resonator," Appl. Phys. B. **31**, 97-105 (1983).
8. D. Hils and J. L. Hall, "Response of a Fabry-Perot cavity to phase modulated light," Rev. Sci. Instrum. **58**, 1406-1412 (1987).
9. E. Morrison, B. J. Meers, D. I. Robertson and H. Ward, "Experimental demonstration of an automatic alignment system for optical interferometers," Appl. Opt. **33**, 5037-5040 (1994).
10. E. Morrison, B. J. Meers, D. I. Roberston and H. Ward, "Automatic alignment of optical interferometers," Appl. Opt. **33**, 5041-5049 (1994).

Table and Figure Captions

Table 1

Parameters of the first and second GEO 600 modecleaners, MC1 and MC2.

Figure 1

Experimental arrangement of the apparatus used to investigate the process of passing modulation sidebands through a modecleaner cavity.

Figure 2

The circuit used to apply modulation sidebands on the light with adjustable frequency f_1. The linewidth of the prototype modecleaner cavity is only 20 kHz. hence in view of the resonance curve of the modulator circuit shown here we may deduce that the variation of applied sideband height is slight over several cavity linewidths.

Figure 3

The amplitude modulation of the transmitted light power as the sideband frequency is varied through the modecleaner cavity FSR.

Figure 4

The appearance relative to the carrier of the applied modulation sidebands (a) on the light entering the modecleaner, (b) on the light exiting the modecleaner when on resonance. The graphs were obtained using a Tropel scanning Fabry-Perot cavity.

Figure 5

A simplified diagram showing the experimental arrangement to investigate the light noise demodulated with respect to f_1. The signals to be spectrum analysed at A and B are those associated with the light after and before the modecleaner.

Figure 6

Traces showing the photodiode signal demodulated at f_1 measured for the light entering and exiting the modecleaner cavity. With a greater span we observed that by several hundred Hz the backgrounds of both traces tend to the measurement shot noise level for the light power used (25 mW): around 10 dB lower than the background level at 100 Hz.

Figure 7

(a) the error signal that would be expected from a theoretical consideration of the cavity response, and (b) the demodulated signal actually measured at point Q over a smaller frequency range.

parameter	MC1	MC2
round trip distance d	8.001 m	8.101 m
free spectral range FSR	37.49 MHz	37.03 MHz
finesse F	1902	1902
linewidth Δf	19.7 kHz	19.5 kHz
corner frequency f_c	9.85 kHz	9.75 kHz
TEM_{nm} mode spacing Δf_{nm}	11.40 MHz	11.37 MHz

Table 1: Parameters of the first and second GEO 600 modecleaners, MC1 and MC2.

Applied Optics: K.D. Skeldon. "Response of a Fabry-Perot optical cavity to phase modulation sidebands ...".

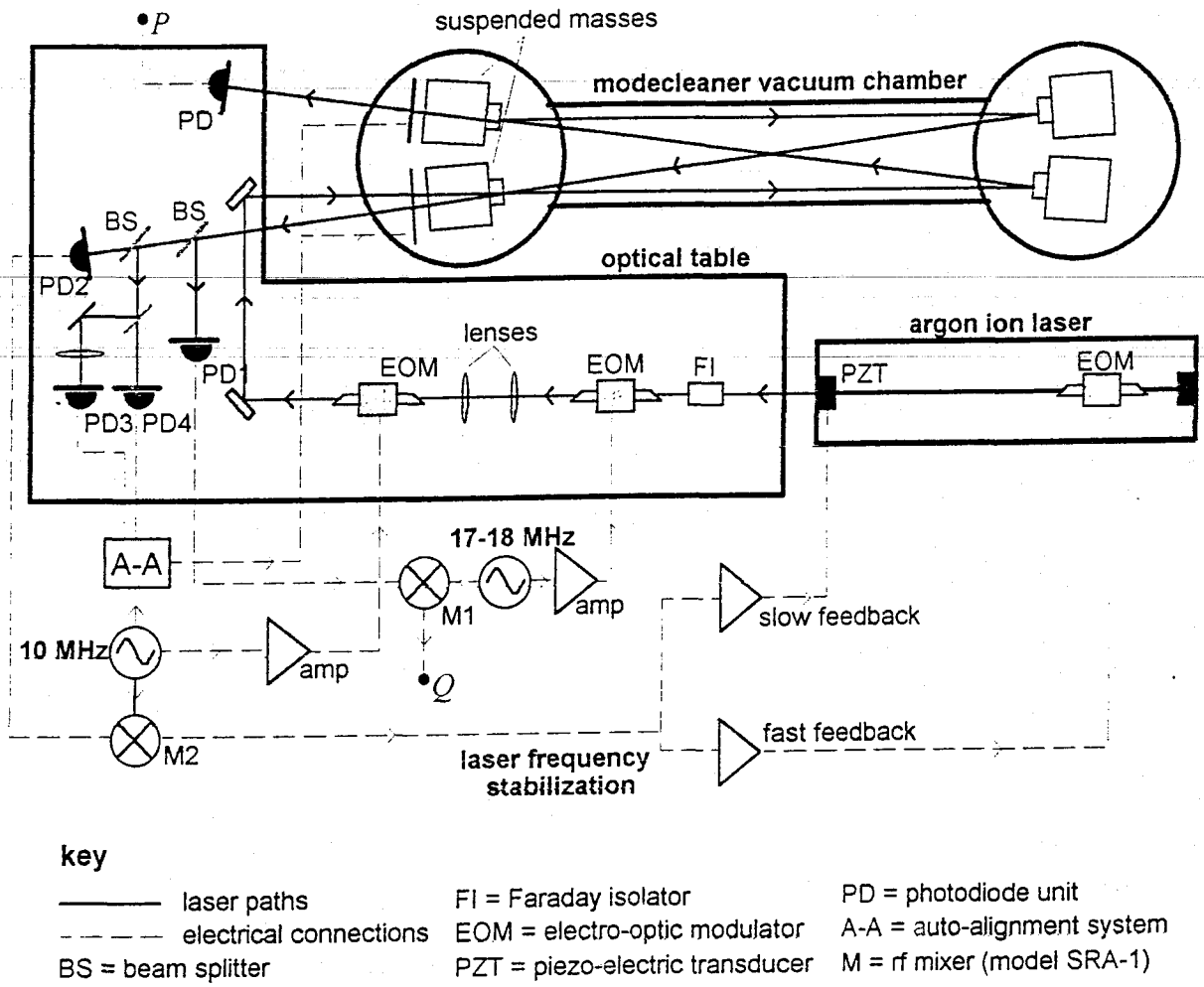

Figure 1: Experimental arrangement of the apparatus used to investigate the process of passing modulation sidebands through a modecleaner cavity.

Applied Optics: K.D. Skeldon, "Response of a Fabry-Perot optical cavity to phase modulation sidebands ...".

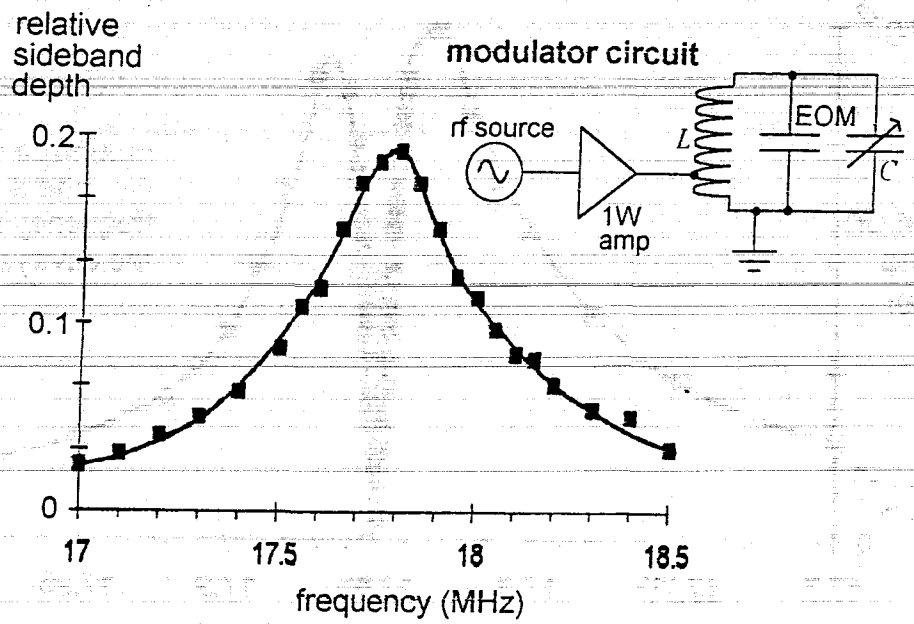

Figure 2: The circuit used to apply modulation sidebands on the light with adjustable frequency f_1. The linewidth of the prototype modecleaner cavity is only 20 kHz, hence in view of the resonance curve of the modulator circuit shown here we may deduce that the variation of applied sideband height is slight over several cavity linewidths.

Applied Optics: K.D. Skeldon, "Response of a Fabry-Perot optical cavity to phase modulation sidebands ...".

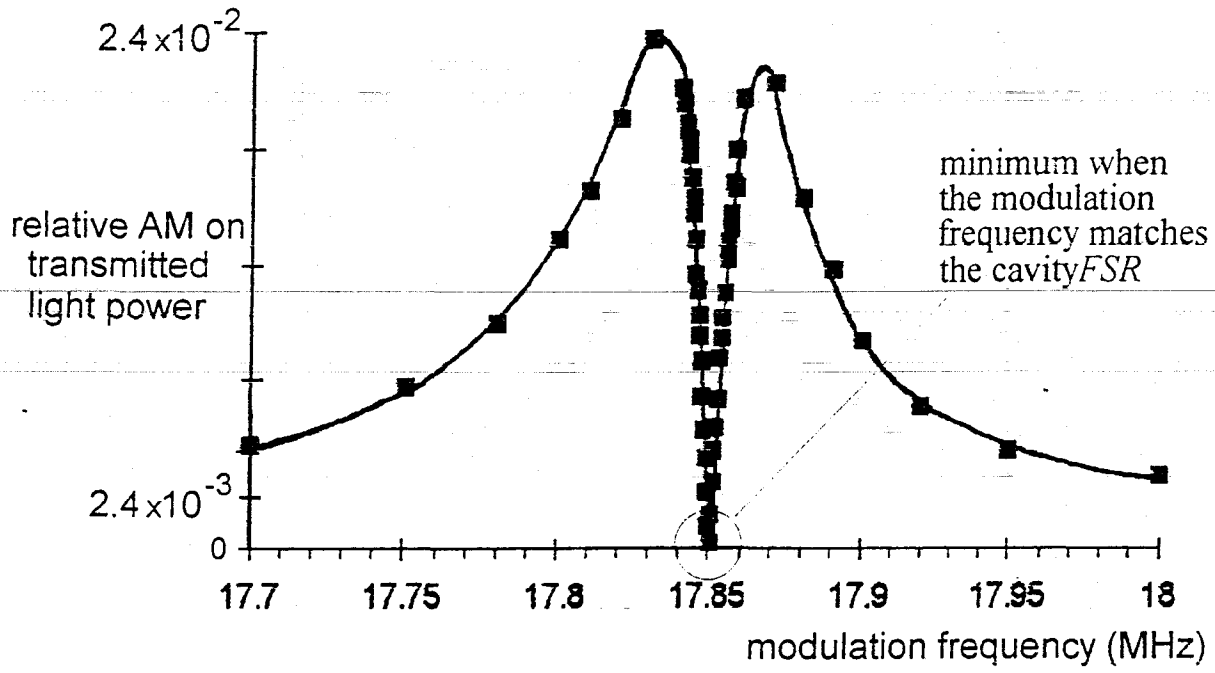

Figure 3: The amplitude modulation of the transmitted light power as the sideband frequency is varied through the modecleaner cavity FSR.

Applied Optics: K.D. Skeldon, "Response of a Fabry-Perot optical cavity to phase modulation sidebands ...".

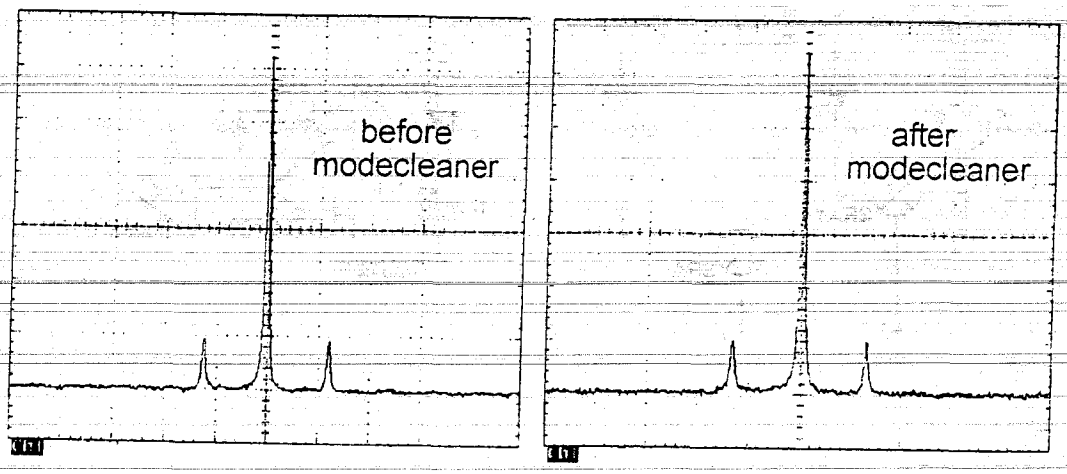

Figure 4: The appearance relative to the carrier of the applied modulation sidebands (a) on the light entering the modecleaner, (b) on the light exiting the modecleaner when on resonance. The graphs were obtained using a Tropel scanning Fabry-Perot cavity.

Applied Optics: K.D. Skeldon. "Response of a Fabry-Perot optical cavity to phase modulation sidebands ...".

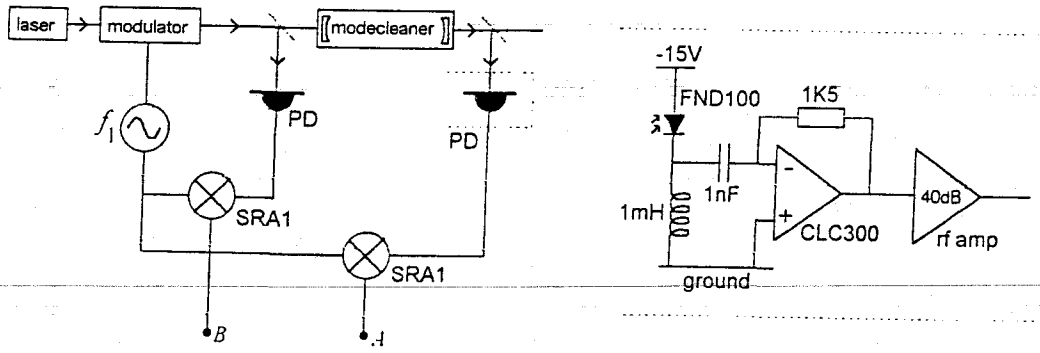

Figure 5: A simplified diagram showing the experimental arrangement to investigate the light noise demodulated with respect to f_1. The signals to be spectrum analysed at A and B are those associated with the light after and before the modecleaner.

Applied Optics: K.D. Skeldon, "Response of a Fabry-Perot optical cavity to phase modulation sidebands ...".

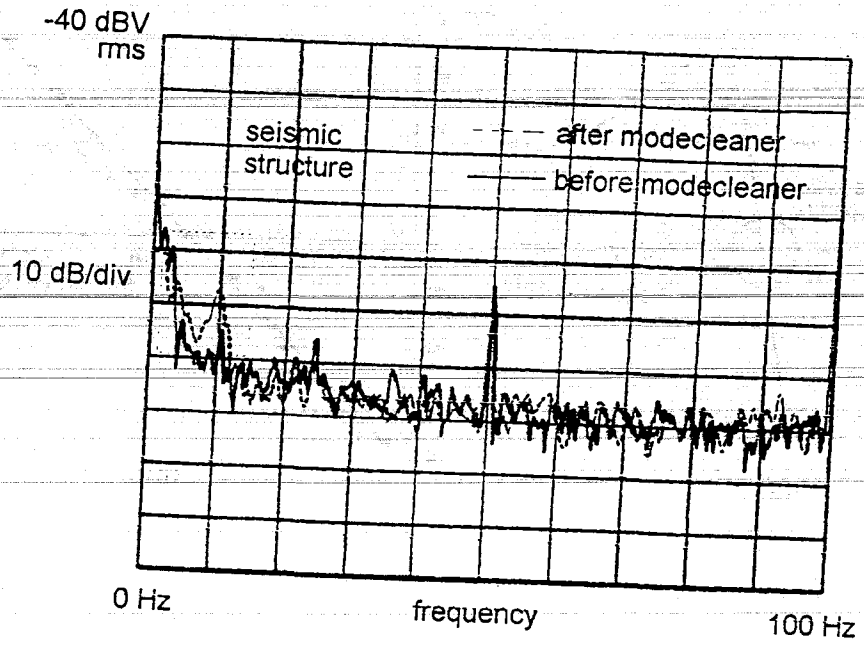

Figure 6: Traces showing the photodiode signal demodulated at f_1 measured for the light entering and exiting the modecleaner cavity. With a greater span we observed that by several hundred Hz the backgrounds of both traces tend to the measurement shot noise level for the light power used (25 mW); around 10 dB lower than the background level at 100 Hz.

Applied Optics: K.D. Skeldon, "Response of a Fabry-Perot optical cavity to phase modulation sidebands ...".

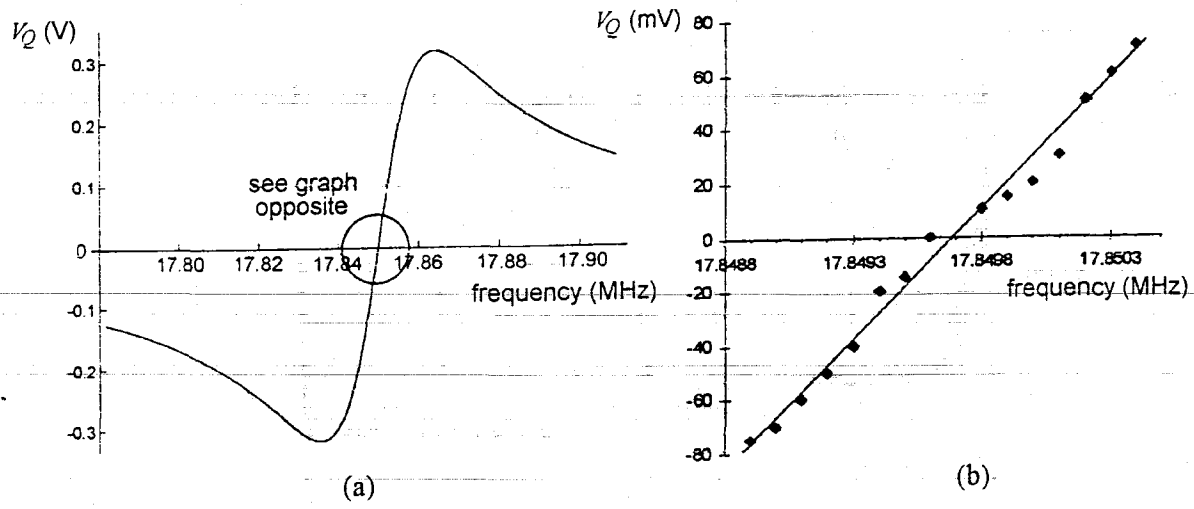

Figure 7: (a) the error signal that would be expected from a theoretical consideration of the cavity response, and (b) the demodulated signal actually measured at point Q over a smaller frequency range.

Applied Optics: K.D. Skeldon, "Response of a Fabry-Perot optical cavity to phase modulation sidebands ...".